Production and Structural Characterization of Some Magnesium Matrix Composites Reinforced with Amorphous/Nanocrystalline NiTi Particulates

MARIANA CIURDAS[1], DANIELA ALINA NECSULESCU[1], CRISTIAN MIRCEA PANTILIMON[1], VASILE ION[2], MAGDALENA GALATANU[3], GEORGE RUIU[3], RUXANDRA ELENA DUMITRESCU[1]*

[1] Politehnica University of Bucharest, Materials Science and Engineering Faculty, 313 Splaiul Independentei, 060042, Bucharest, Romania

[2] Politehnica University of Bucharest, Engineering and Management of Technological Systems Faculty, 313 Splaiul Independenţei, 060042, Bucharest, Romania

[3] National Institute of Materials Physics, 405 A Atomistilor Str., 077125, Magurele, Ilfov Romania

Two mixtures of elemental nickel and titanium powders in atomic proportions of 50% Ni + 50% Ti and 32% Ni + 68% Ti, respectively, were ground for 40 hours in a high energy planetary mill. In the case of the first mixture, the mechanical alloying was totally produced, while for the second, the alloying was partial. In both mixtures, qualitative X-ray diffraction phase analysis revealed the presence of metastable phases, such as Ni HC and NiTi- R-phase. Also, the equiatomic mixture is characterized by a partially amorphous structure. 10% of each type of mixture submitted to milling was used as reinforcing element in the form of particulates for two magnesium matrix composites. They were obtained by sintering in the plasma at 590°C. In the case of the reinforced with the second mixture composite, the production of new phases other than the matrix and those present in the mixture of nickel and titanium powders after milling were recorded. The electron microscopy images of the two composites have resistant, free of micropores or microcracks matrix / particulates interfaces. The Mg-10% (32 at% Ni + 68 at% Ti) composite is characterized by Vickers hardness higher than that of the composite reinforced with the equiatomic mixture.

Keywords: amorphous / nanocrystalline NiTi reinforcement, mechanical alloying, magnesium matrix, spark plasma sintering

Numerous researchers have studied the near-equiatomic NiTi alloy, characterized by a remarkable shape memory effect, superelasticity, several compositions exhibiting also biocompatibility [1,2]. Relatively recently, the NiTi equiatomic alloy with amorphous or partially amorphous (amorphous/nanocrystalline) structure has also raised an interest as a potential reinforcement element for light metal matrices (Al, Mg) [3]. Other alloys were suggested as reinforcement elements, such as some easily amorphizable alloys from Fe-B-Si-Nb, Fe-Co-B-Si-Nb, Mg-Cu-Zn-Y, Cu-Zr-Ti, Zr-Nb-Cu-Ni-Al, etc. [4]. The usage of amorphous particulates or metallic glass ribbons as reinforcement element instead of the usual ceramic particulates/fibres presents several advantages, including:

-matrix / reinforcement interface characterized by a better resistance, due to the fact that both the matrix and the dispersed phase are metallic materials;

-high mechanical strength characteristics without drastic decrease of plasticity.

In the present paper, two magnesium composites reinforced with NiTi alloy particulates obtained by mechanical alloying of nickel and titanium powders in the proportions: 32 at % Ni / 68 at % Ti and 50 at % Ni / 50% at Ti were obtained and characterized as for the microstructure. The mechanical alloying and amorphization capacity of the two powder blends, milled under identical conditions, was also analyzed.

Experimental part
Materials and methods

The production of the amorphous / nanocrystalline metal matrix composites with amorphous / nanocrystalline metal particles was accomplished in two steps, respectively:

I. obtaining the complementary particulate material by mechanically alloying of the elemental nickel and titanium powders;

II. manufacture of magnesium matrix composites by spark plasma sintering (SPS).

I. Of the elementary nickel and titanium powders (Alfa Aesar), having the dimensions of 44µm and 100µm, respectively, two mixtures were weighed whose chemical composition are shown in table 1. They were encapsulated under argon atmosphere and ground for 40 h in a Retsch PM 400 high energy planetary mill at a rotational speed of 250 rpm. The grinding balls were of 15 mm in diameter and the ball / powder mass ratio was of 7 : 1.

The phase composition of the four powder mixtures was determined by X-ray diffraction, using a PANalytical X'PERT Pro diffractometer with copper anticathode.

II. The powders A1 and B1 were the reinforcement element, in a proportion of 10 wt%, for two pure magnesium matrix composites. The composites were obtained from the solid state by powder metallurgy specific processes. In this regard, magnesium powder with an average particle size of 74 µm, supplied by Alfa Aesar was used for the

Sample Code	Chemical composition of powder mixtures or		Number of grinding hours
	Atomic %	Weight %	
A0	32% Ni, 68% Ti	37% Ni, 63% Ti	-
A1			40
B0	50% Ni, 50% Ti	45% Ni, 55% Ti	-
B1			40

Table 1
CHEMICAL COMPOSITION OF POWDER MIXTURES SUBMITTED TO GRINDING

* email: ruxandraelenadumitrescu@gmail.com; Phone: +40723344813

matrix. The magnesium powders as well as the nickel and titanium ones corresponding to samples A1 and B1 were manually homogenized for 15 min and then sintered under argon atmosphere using the SPS technique (sintering furnace FCT Systeme D50). The sintering cycle operated at a maximum temperature of 590° C, holding time of 8 minutes, and a compaction force of 5 kN. Heating was performed in two steps, up to 460° C, with a heating rate of 140°C/min., and up to 590°C with a heating rate of 40° C/min. The cooling rate was of 190° C/min.

Structural characterization of magnesium matrix composites was performed by X-ray diffraction using a PANalytical X'PERT Pro diffractometer with copper anticathode and scanning electron microscopy, with a SEM QUANTA FEG 450 microscope.

Vickers hardness testing of magnesium matrix composites reinforced with 10% A1 and 10% B1, respectively, was performed with a Shimadzu HMV-2 Series durometer using a 1,961 N (HV0,2) force for 15 seconds. Five measurements per sample have been made, with a distance of 0.5 mm between fingerprints.

Results and discussions
Reinforcement materials analysis

The diffraction spectra of samples A0, A1, B0 and B1 are shown in figures 1 and 2.
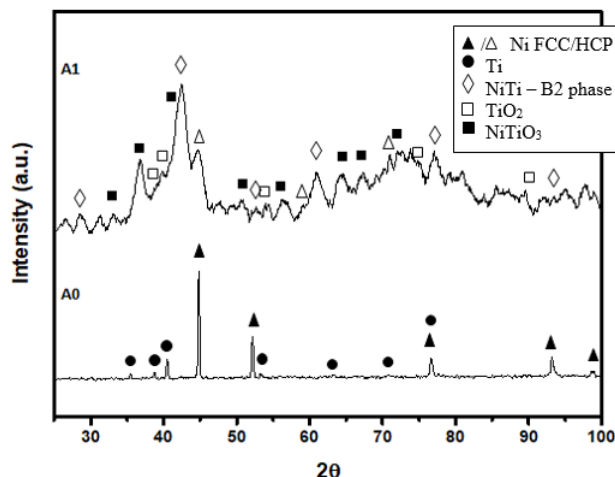

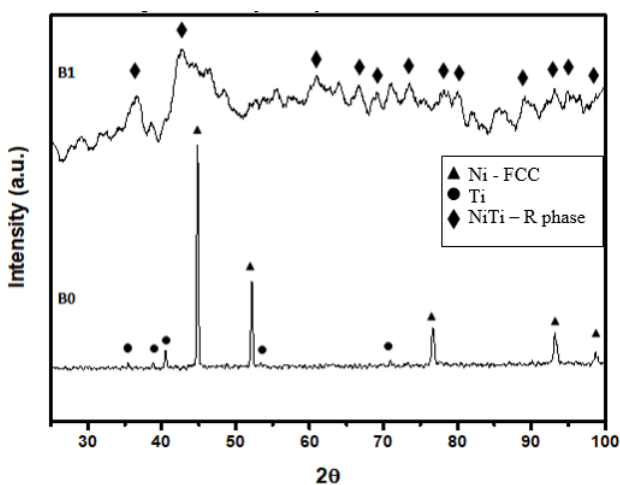Fig. 1. Diffraction spectra of powder mixtures A0 and A1

Fig.2. Diffraction spectra of powder mixtures B0 and B1

One can see from figures 1 and 2 that the diffraction spectra of samples A0 and B0 reveal the representative lines of nickel and titanium, respecting their relative intensities. It is also highlighted the raise of titanium-specific lines intensities in sample A0 as compared to sample B0, corresponding to a higher proportion of titanium.

Qualitative analysis by X-ray diffraction of sample A1 (upper side, fig. 1) and sample B1 (upper side, fig. 2) confirms the presence of the following phases: NiTi - B2 Phase, TiO_2 and $NiTiO_3$ oxides as well as pure Ni in sample A1 and NiTi - R phase in sample B1.

The nickel present in sample A1 exhibits compact hexagonal lattice and is a phase reported in many works as metastable [5 - 8]. Its existence indicates that the mechanical alloying of the Ni32Ti68 powder mixture was incomplete. The formation of nickel with a HC structure and not a FCC one, after a 40h grinding, is due to the processes and phenomena developed during mechanical alloying in high energy mills (powder fragmentation, severe deformation, cold welding, etc.). In this respect, it is well-known that the mechanical alloying of elemental powders or pulverulent master alloys produces non-equilibrium, metastable, amorphous or quasi-crystalline phases [9].

Titanium oxide and nickel titanate are formed in sample A1 and do not appear in sample B1, most likely their quantity being in this latter sample below the detection limit of the diffractometer. The presence of oxides in sample A1 is due to the high proportion of titanium as against nickel. Characterized by high reactivity titanium easily oxidizes, the reaction being strongly exothermic, which results in an additional local increase in temperature in the vial. This favors the oxidation of nickel powders and the formation of titanate.

The characteristic diffraction lines of B2 phase, along with those of nickel, confirm the partial accomplishment of mechanical alloying, while the exclusive presence of the R phase in sample B1 demonstrates the full production of this phenomenon. The R - phase was obtained in sample B1 as a metastable phase [10]; the transformation B2→R is favored both by the formation of a nanocrystalline structure and by the strong deformation of the powder particulates, both phenomena being specific to grinding [11,12]. In case of sample A1, strong exothermic reactions contribute to raising the temperature at microscopic level and suppress transformation B2→ R [13, 14].

As for the sample B1 diffraction spectra aspect (the main peak of the NiTi phase is largely widened, the diffracted radiation intensity is low) the presence of an amorphous phase proportion can be estimated. In sample A1 one can see also a widening of the peaks and a decrease in the diffraction radiation intensity, but the diffraction lines appearance indicates rather a decrease in the crystallites sizes until a nanocrystalline structure is obtained and not the amorphization of a part of the structure. In this respect, specific quantitative assessments of the amorphous proportion of the structure are required. The absence or the presence of a very small proportion of the amorphous phase in sample A1 was expected since the formation of oxides are subsequent to highly exothermic reactions, which caused a significant local temperature increase.

Composites analysis

The microstructural characterization of the two magnesium matrix composites reinforced with the A1 and B1 (10% A1 in Mg and 10% B1 in Mg, respectively) powders was performed by X-ray diffraction and electron microscopy.

The diffraction spectra of the Mg + 10% A1 and Mg + 10% B1 composite samples are shown in figures 3 and 4.

Qualitative phase analysis reveals the existence of the following phases: Mg, NiTi - B2 phase, $NiTi_2$, Mg_3Ni_3Ti and $NiTiO_3$ in Mg + 10% A1 (fig. 3) and Mg and NiTi - B2 phase in Mg + 10% B1, respectively (fig. 4). Many researchers have reported the simultaneous presence of NiTi, $NiTi_2$ and Ni_3Ti phases after sintering or heat treatment of Ni and Ti

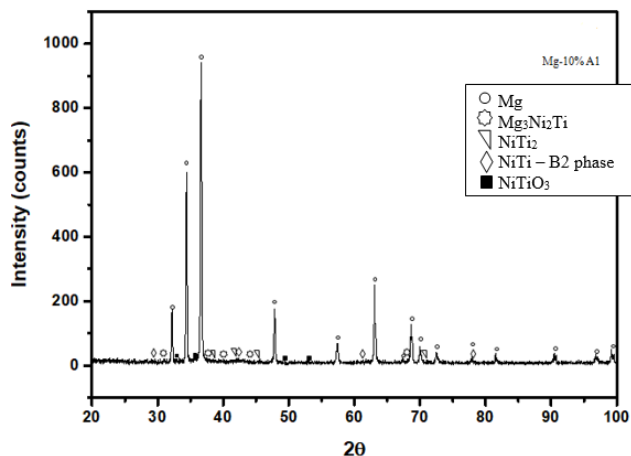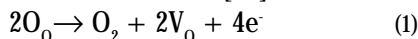Fig. 3. Mg + 10% A1 composite diffraction spectrum

Fig. 4. Mg + 10% B1 composite diffraction spectrum

powders after previous milling [15-17]. The plasma sintering process, through its high heating/cooling rates, minimizes the rate of decomposition of the NiTi compound [18]. However, the $NiTi_2$ phase is identified in the Mg + 10% A1 diffraction spectrum -although the complementary material quantity is small - only 10% - and is not present in the sample analysis Mg + 10% B1 (either below the apparatus detection limit, or it does not form at all in this sample).

Formation of $NiTi_2$ and Mg_3Ni_2Ti phases in the Mg + 10% A1 sample takes place in the sintering process and is due to titanium oxides and nickel and titanium oxides, respectively, present in the reinforcement powder. The point defects present in the oxides represent an oxygen source according to the reduction reaction [19]:

$$2O_O \rightarrow O_2 + 2V_O + 4e^- \qquad (1)$$

where:

O_O - oxygen ion occupying a normal position in the node of the crystalline lattice;

V_O - vacancy resulting from leaving the node occupied by an oxygen ion (with a load of +2 relative to the interstitial lattice of oxygen ions);

Additionally, it is known that during spark plasma sintering (SPS), there is an increase in the density of point defects [20, 21]. Thus, oxygen intake favors the simultaneous existence of NiTi, $NiTi_2$ and Ni_3Ti, requiring phase balance analysis in the Ni-Ti-O system and not in the Ni-Ti system [22], despite the high heating/cooling rates and short compaction time, characteristic for plasma sintering.

According to the Ni-Ti-O ternary equilibrium diagram, in the isothermal section at 900°C - temperature that can be reache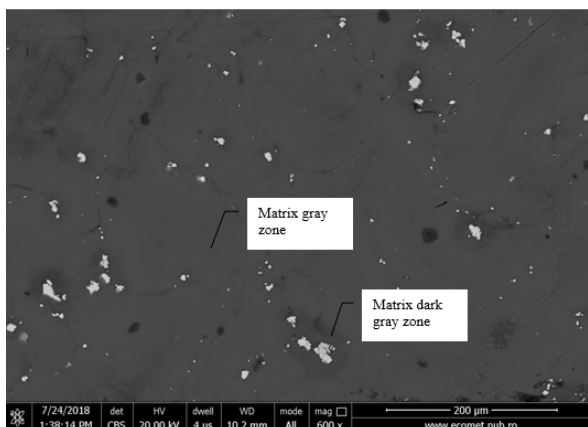d inside the sample during sintering [9] - there is a relatively large NiTi + Ni_3Ti + $NiTi_3$ ternary range whereas the NiTi monophasic domain is narrower than the previous one, corresponding to a reduced oxygen concentration. This is the reason why only NiTi lines appear in the Mg+10% B1 composite.

The formation of the Mg_3Ni_2Ti compound is favored by the SPS technique and can be carried out according to the reaction [23]:

$$6Mg + NiTi + Ni_3Ti \rightarrow 2Mg_3TiNi_2 \qquad (2)$$
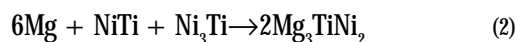
Since NiTi is found in a higher proportion than Ni_3Ti, most likely the above reaction completely consumed the nickel-rich compound, fact confirmed by the presence of NiTi phase characteristic lines and by the absence of the Ni_3Ti specific diffraction lines (fig. 3).

The sintering temperature of 590°C is high enough for suppressing the R- phase transformation, thus only the NiTi - B2 phase lines, obviously along with the magnesium ones, are identified in the Mg-10% B1 sample (fig. 4).

The scanning electron microscopy images of the two composites are shown in figures 5 and 6. The reinforcement element particulates appear as being white on a gray background, the latter being the magnesium matrix. Black micropores are found in both samples, in a higher volume ratio in B1 sample (fig. 6). In both samples, a continuous and thus presumably resistant matrix / reinforcement element interface is seen, lacking pores or microcracks.

One may see in the figure 5 micrograph some darker matrix areas (dark gray) surrounding the reinforcement particulates, while the micrograph of the Mg-10% B1 sample does not reveal such formations around them.
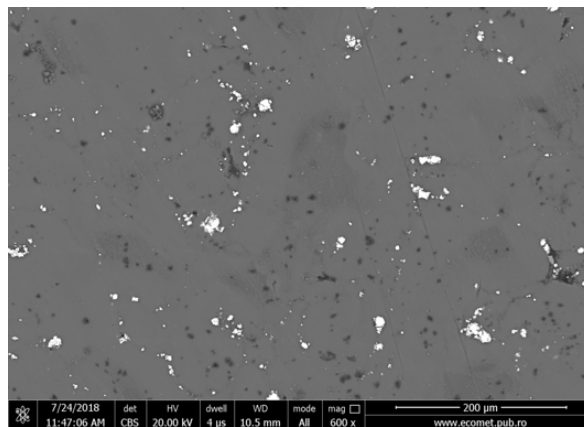

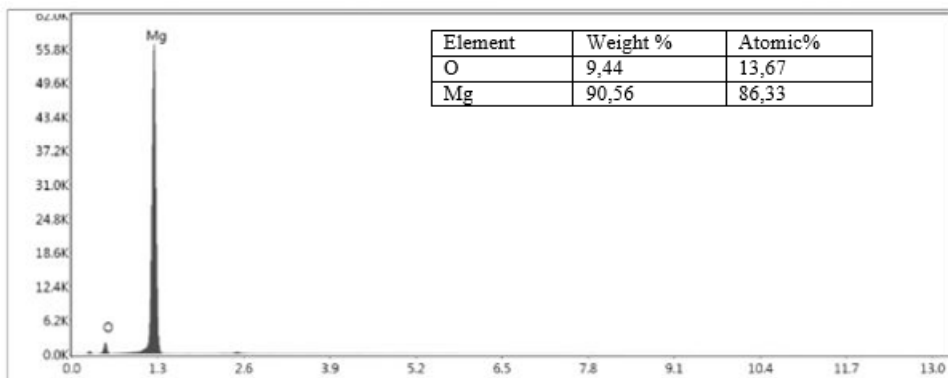Fig. 5. Scanning electron microscopy (BSE) image of Mg-10% A1

Fig. 6. Scanning electron microscopy (BSE) image of Mg-10% B1

Element	Weight %	Atomic%
O	9,44	13,67
Mg	90,56	86,33

Fig. 7. EDS analysis of the dark gray area found in the magnesium matrix of the Mg-10% A1 sample

Element	Weight %	Atomic%
O	5,04	7,79
Mg	94,96	92,21
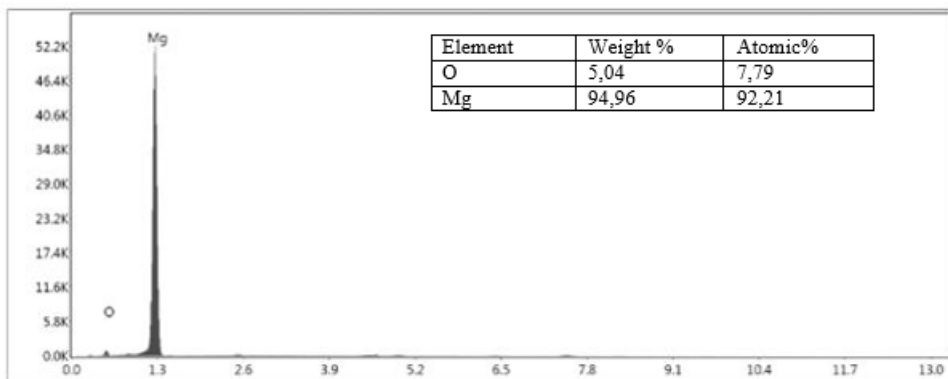
Fig. 8. EDS analysis of the gray area found in the magnesium matrix of the Mg-10% A1 sample

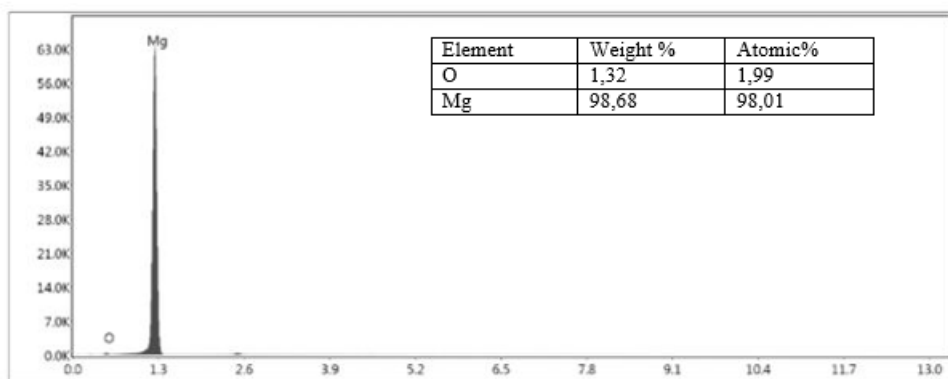| Element	Weight %	Atomic%
O	1,32	1,99
Mg	98,68	98,01

Fig. 9. EDS analysis of the magnesium matrix of the Mg-10% B1 sample

The EDS analysis of dark gray and gray areas, respectively, in the Mg-10% A1 sample matrix as well as the Mg-10% B1 sample matrix is shown in figures 7-9.

It is found that around the reinforcement element particulates A1 there is a higher content in oxygen zone than the rest of the matrix (9.44% O versus 5.04% O (figs. 7 and 8). This is attributed to an oxygen diffusion provided by the multiplication of point defects described by reaction (1), diffusion made from the reinforcement element towards the matrix during sintering.

Practically the magnesium matrix is additionally oxidized, the oxygen source being an *internal* one, represented by the reinforcement element. In the case of the sample reinforced with 10% B1, the oxygen proportion is lower (fig. 9) and is due to the oxidation of the magnesium powder during the homogenization performed prior to the sintering process.

The stronger oxidation of the matrix reinforced with 10% A1 composite resulted in a slightly higher hardness as compared to that of the reinforced composite with 10% B1. The composite hardness values are shown in table 2. For sake of comparison, the hardness of pure magnesium obtained by sintering under the same conditions is also given.

Table 2
VICKERS HARDNESS OF REINFORCED COMPOSITES WITH 10% A1 AND B1, RESPECTIVELY

Sample	HV0,2
Mg	35.8
Mg-10% A1	37.9
Mg-10% B1	41.4

Conclusions

Elementary Ni and Ti powders in various proportions: 32 at % Ni/68 at % Ti - sample A1 and 50 at % Ni/50 at % Ti - sample B1, respectively, were milled for 40 h in a high energy planetary mill. In the case of the equiatomic mixture (sample B1), the mechanical alloy was complete, thus the NiTi compound was obtained. In sample A1, the mechanical alloying was partial because the pure nickel was also found in the phase composition. In both blends of 40 hour milled powders, metastable phases, such as NiTi - R phase (sample B1), Ni-HC (sample A1), are found. One can also observe the presence of oxides (TiO_2 and $TiNiO_3$) formed in the A1 mixture, most likely due to a higher amount of titanium which has oxidized during milling before the mechanical alloying. They do not appear in sample B1,

most likely being below the detection limit of the diffractometer.

Two magnesium matrix composites reinforced with 10% of A1 and B1 particulates mixtures were obtained by plasma sintering at 590°C.

The phase composition of the Mg-10% A1 composite, established by X-ray diffraction, reveals Mg_3TiNi_2 and $NiTi_2$ compounds lines along with the characteristic lines of Mg, NiTi and $NiTiO_3$. Formation of the $NiTi_2$ and Ni_3Ti phases is favored by the presence of oxides and the ternary compound is most likely obtained by a reaction between Mg, $NiTi_2$ and Ni_3Ti until the latter is consumed. In the Mg-10% B1 composite only the Mg and NiTi phases are found.

Both composites have a clean matrix/reinforcement element interface, lacking microporosities or microcracks, as seen from scanning electron microscopy images. In the case of the composite Mg-10% A1, darker matrix microzones surrounding the reinforcing element particulates are found. EDS analysis confirmed that these microzones are more oxygen-rich than the rest of the matrix. This additional oxidation of the matrix may be responsible for the slightly higher hardness of the Mg-10% A1 composite.

The two composites are characterized by a higher hardness than that of the pure magnesium obtained by sintering under the same conditions.

References

1.GHERGHESCU, I.A., JICMON, G.L., BRANZEI, M., TARCOLEA, M., CIUCA, S., Re. Chim. (Bucharest), **67**, no. 2, 2016, p. 306.
2.GHERGHESCU, I.A., JICMON, G.L., COTRUT, C., BRANZEI, M., BERBECARU, A.C., PREDESCU, A.M., CIUCA, S., Rev. Chim.(Bucharest), **67**, no. 9, 2016, p.1736.
3.SANKARANARAYANAN, S., HEMANTH SHANKAR, V., JAYALAKSHMI, S., NGUYEN, Q. B., GUPTA, M., J ALLOY COMPD, **627**, 2015, p. 192.
4.JAYALAKSHMI, S., SANKARANARAYANAN, S., GUPTA, M., METALS, **5**, no. 2, 2015, p. 743.
5.TZITZIOS, V., BASINA, G., GJOKA, M., ALEXANDRAKIS, V., GEORGAKILAS, V., NIARCHOS, D., BOUKOS, N., PETRIDIS, D., NANOTECHOLOGY, **17**, no. 15, 2006, p. 3752.
6.HE, L., J MAGN MAGN MATER, **322**, no. 14, 2010, p. 1992.
7.KAPAKLIS, V., PAPPAS, S.D., POULOPOULOS, P., TRACHYLIS, D., SCHWEISS, P., POLITIS, C., J NANOSCI NANOTECHNOL, **10**, no. 9, 2010, p.6024.
8.GARCIA-CERDA, L.A., BERNAL-RAMOS, K.M., MONTEMAYOR, S.M., QUEVEDO-LOPEZ, M.A., BETANCOURT-GALINDO, R., BUENO-BAQUES, D., J NANOMATER, 2011, Article ID 162495.
9.SURYANARAYANA, C., PROG MATER SCI, **46**, no. 1-2, 2001, p. 79.
10.GHERGHESCU, I.A., TARCOLEA, M., JICMON, G.L., TURCAS, C.V., Rev. Chim. (Bucharest), **64**, no. 4, 2013, p. 53.
11.KHALATBARI, M.S, DANESHPOUR, M, NANOMED RES J, **2**, no. 4, 2017, p. 267.
12.SHI, X., CUI, L., JIANG, D., YU, C., GUO, F., YU, M., LIU, Y., J MATER SCI, **49**, no. 13, 2014, p. 4643.
13.GONZALEZ, C.H., OLIVEIRA, C.A.N., PINA, E.A.C., URTIGA FILHO, S.L., FILO, O.O.A, DE ARAUJO, C.J., MAT RES, **13**, no. 3, 2010, p. 325.
14.KUS, K., BRECZKO, T., MATER PHYS MECH, **9**, 2010, p. 75.
15.MOUSAVI, T., KARIMZADEH, F., ABBASI, M. H., MATER SCI ENG, A, **487**, no. 1-2, 2008, p. 46.
16.SADEGHI, A.R., MOSTAJABODAVEH, H., BABAKHANI, A., ABRAVI, M. S., SALEHI, A., J WUHAN UNIV TECHNOL, **32**, no. 5, 2017, p. 1156.
17.MARTINS, C.B., FERNANDES, B.B., RAMOS, E.C.T., SILVA, G., RAMOS, A.S., MATER. SCI. FORUM, **530-531,** 2006, p. 217.
18.FARVIZI, M., KAHKHAEI JAVAN, M., AKBARPOUR, M.R., KIM, H.S., CERAM INT, **44**, no. 13, 2018, p. 15981;
19.ALEXANDER, J.C., Surface Modifications and Growth of Titanium Dioxide for Photo-Electrochemical Water Splitting, Springer Theses, Springer International Publishing Switzerland 2016, p. 303-306.
20. GUILLON, O. , GONZALES-JULIAN, J., DARGATZ, B., KESSEL, T., SCHIERNING, G., RATHEL, J., HERRMANN, M., ADV ENG MATER, **16**, no. 7, 2014, p.830.
21.MUNIR, Z.A., ANSELMI-TAMBURINI, U., OHYANAGI, M., J. MATER. SCI., **41**, no. 3, 2006, p. 763;
22.CHUPRINA, V.G., SHALYA, I.M, POWDER METALL MET CERAM, **41**, no. 1-2, 2002, p. 85;
23.DENYS, R.V., ZAVALIY, I.YU., BEREZOVETS, V.V., PAUL-BONCOUR, V., PECHARSKY, V.K., Intermetallics, **32**, 2013, p. 167.